RESEARCH ARTICLE

Quantifying the Early Stages of Remyelination Following Cuprizone-induced Demyelination

Mark F. Stidworthy[1]; Stephane Genoud[2]; Ueli Suter[2]; Ned Mantei[2]; Robin J. M. Franklin[1]

[1] Department of Clinical Veterinary Medicine and Cambridge Centre for Brain Repair, University of Cambridge, United Kingdom.
[2] Institute of Cell Biology, ETH Hönggerberg, Zürich, Switzerland

The demyelinating toxin cuprizone is used increasingly in mouse studies of central nervous system remyelination. The value of this model for such studies depends on an accurate description of its quantifiable features. We therefore investigated histology and ultrastructure during the early oligodendrocyte differentiation phase of remyelination in mice given cuprizone and allowed to recover for 2 weeks. Limiting the dose of cuprizone to 0.2% overcame significant mouse morbidity and weight loss seen with a 0.4% dose, but the distribution of cuprizone-induced demyelination was anatomically variable. The caudal corpus callosum and dorsal hippocampal commissure mostly demyelinated at this dose, but the rostral corpus callosum and rostral cerebellar peduncles did not. This variable response, together with small axon diameters and hence thin myelin sheaths, hindered analysis of the progress of early remyelination. The proportion of myelinated and unmyelinated axons in defined regions followed expected trends, but there was pronounced variation between animals. Furthermore, group mean G ratios did not change as expected during the early stages of remyelination, and regression analysis revealed a complex relationship between axon diameter and myelin sheath thickness during this period. We also noted axonal pathology that persisted for at least 2 weeks after cuprizone withdrawal.

Brain Pathol 2003;13:329-339.

Introduction

There is accumulating evidence to suggest that a subset of chronically demyelinated lesions in multiple sclerosis contain oligodendrocyte progenitors which fail to differentiate into myelin sheath forming cells (8, 9, 26, 27). In this context, the process of oligodendrocyte differentiation and maturation, by which immature cells develop the capacity to interact with demyelinated axons and invest them with new myelin sheaths, has assumed an increasing importance in the search for new experimental and therapeutic approaches to enhance remyelination.

With the burgeoning of knock-out, transgenic and conditional transgenic mice, there are increased opportunities to investigate the roles of a range of factors that might influence this process. Consequently, there has been a renewed interest in murine models capable of delivering reliable and consistent demyelination and remyelination in defined white matter tracts without excessive morbidity and mortality. However, identifying suitable models is not straightforward. Despite its technical demands, and some surgical morbidity, the direct injection of gliotoxins into the CNS has proved a reliable and reproducible method of inducing focal demyelination in large diameter myelinated fiber tracts in rats (28). Nevertheless, in mice, stereotaxic lesioning of specific white matter tracts in the brain is difficult, and achievable lesion sizes small, making this technique better suited to rats. Recently, studies in mice have shown a renewed interest in the use of cuprizone as a toxic model of demyelination (22). This seems a promising approach since cuprizone can be delivered easily mixed into food, and is reported to produce reliable demyelination of specific central white matter tracts such as the corpus callosum. In this study we examine the suitability of the cuprizone model for the investigation of early remyelination events in transgenic mice.

The sequence of events in cuprizone intoxication has been reviewed (22), and although the exact mechanism of action remains unclear, follows a consistent pattern. Loss of myelin and oligodendrocytes during the first three weeks of cuprizone administration is followed by recruitment of microglia, macrophages and astrocytes, together with the proliferation of oligodendrocyte progenitors, such that after 5 or 6 weeks of continuous cuprizone administration, demyelination is maximal and remyelination begins. Withdrawal of cuprizone at this stage results in significant remyelination over the course of about 4 weeks. In the face of continued cuprizone administration however, successive waves of demyelination continue and a chronically demyelinated state may be reached (18, 19).

Recent studies (15, 24) have selected the corpus callosum as the site for the analysis of post-cuprizone

Corresponding author:
Robin J.M. Franklin, Department of Clinical Veterinary Medicine, University of Cambridge, Madingley Road, Cambridge, CB3 0ES, United Kingdom (e-mail: rjf1000@cam.ac.uk)

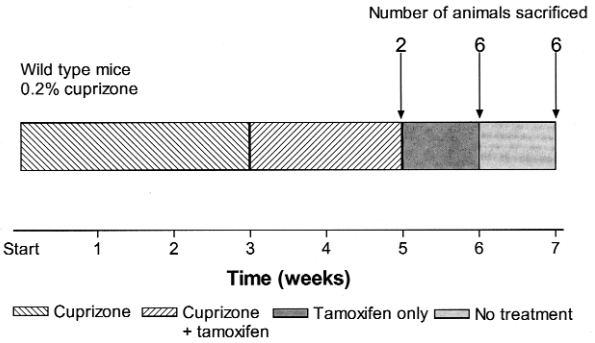

Figure 1. Schematic of the experimental protocol to investigate the effects of cuprizone on remyelination in wild type transgenic mice.

remyelination, in contrast to earlier studies which used the rostral cerebellar peduncle (4, 17). In the latter, the majority of axons are of a larger diameter, with the result that the alterations in myelin thickness resulting from demyelination and remyelination are readily recognized, which may not be the case in the corpus callosum. Furthermore, the earlier protocols fed high doses of cuprizone to weanling mice, and even higher doses to old mice (6), whereas current protocols use a reduced dosage fed to adult mice. The purpose of this is to reduce morbidity in treated mice. However, the evidence suggests that the balance between efficacy in demyelination and toxicity is fine. There is variability in the sensitivity of different strains and ages of mice to both the demyelinating and toxic effects of cuprizone (10, 17), and dosage regimens must be titrated accordingly (15).

In the search for a suitable model in which to investigate factors influencing the differentiation and maturation of oligodendrocyte progenitors we evaluated the earliest stages of the remyelination response following cuprizone demyelination of the corpus callosum of adult mice. In particular, we have examined the value of using the corpus callosum as a substrate for the investigation of early remyelination events, in relation to the anatomical features of the site (such as myelinated fiber size and distribution) and in terms of the uniformity of the remyelination response to cuprizone demyelination. We assessed the extent of demyelinating changes across the corpus callosum and adjacent myelinated tracts, the proportions of myelinated axons regaining myelin sheaths in defined areas, and most importantly, the way in which new myelin sheaths were laid down on putative remyelinating axons, as measured by the G ratio (the ratio of axon diameter to the fiber diameter of axon plus myelin sheath). This study has revealed a number of unexpected and important factors that bear upon the analysis of remyelination studies using these low doses of cuprizone for analysis of the corpus callosum.

Materials and Methods

Cuprizone administration and tissue processing. In order to determine a dose regimen with manageable levels of morbidity and mortality, groups of normal 10-week-old C57Bl/6 mice were given 0.2% (n=8 females, 7 males) or 0.4% (n=8 females, 8 males) by weight cuprizone (bis-cyclohexanone oxaldihydrazone) mixed into a standard powdered rodent chow. The use of older mice is suggested to increase reproducibility and minimize toxic effects (22). In addition age matched animals (n=4 females and 4 males) received standard powdered chow without cuprizone. The cuprizone-containing diet was maintained for 5 weeks during which time animals were weighed weekly.

As a result of the dosage experiment, it was apparent that a dose of 0.2% cuprizone was the maximum that would be acceptable in terms of levels of morbidity and regulatory limits for weight loss during an experiment. Consequently, a group of 12-week-old mice of C57Bl/6;129 genetic background, suitable to act as wild-type controls in a conditional knock-out transgenic mouse study were given 0.2% by weight cuprizone mixed into a standard powdered rodent chow. The protocol is summarized in Figure 1. Animals were acclimatized to the powdered food without cuprizone for a few days prior to its addition to the diet, and then maintained continuously on the cuprizone-containing diet for 5 weeks, being weighed daily. They were then returned to a normal diet for up to 2 further weeks. In addition, from the end of the third week until the end of the sixth week, each mouse received one μg of tamoxifen by intraperitoneal injection daily, to mimic an oestrogen sensitive induction protocol for recombination in genetically modified lox-CreER transgenic mice. At the end of the fifth, sixth, or seventh weeks from the beginning of cuprizone administration animals (n=2, 6, and 6 respectively) were terminally anesthetized with pentobarbitone and perfused for 10 minutes with 4% glutaraldehyde in phosphate buffer via the left ventricle. In addition, 4 normal age-matched C57Bl/6 mice were processed similarly for comparison. Brains were removed and post-fixed for at least 48 hours. Each brain was then bisected sagittally through the midline, and 2 para-sagittal slices of one mm thickness prepared and trimmed using a metal mouse brain matrix (Agar Scientific). Tissue blocks were trimmed to encompass the

regions of interest, and then processed through osmium tetroxide, dehydrated and embedded in TAAB resin. One-μm sections were cut and stained with alkaline toluidine blue. Selected blocks were trimmed and ultrathin sections cut for electron microscopy.

Histological and morphometric analysis. Toluidine blue-stained sections from 3 regions of the brain were observed. These sections were *i)* midline sagittal section including the entire corpus callosum, subjacent ventricle and rostral commissure; *ii)* para-sagittal section 1mm laterally, encompassing the hippocampus, dorsal hippocampal commissure and corpus callosum; and *iii)* midline sagittal section of the midbrain and hind brain, including the decussation of the rostral cerebellar peduncle. A single observer made a qualitative assessment of the myelination status of white matter tracts in blinded sections from each animal. The distribution of changes was drawn onto a standard pro forma diagram that was subsequently used to generate a distribution map. In addition for the 6- and 7-week time points, white matter tracts within blinded sagittal and para-sagittal sections were ranked independently for myelination by the same observer, and rank orders compared using the Wilcoxon rank sum test.

For morphometric analysis, at least 50 myelinated axons were measured from each of 2 sites in the corpus callosum, again by a blinded observer, from one mouse at the 5-week, 3 mice each at the 6- and 7-week time points (selected from the top, middle and bottom of the rankings), and from the 4 normal C57Bl/6 mice. Using a fixed magnification (12 000×), 10 electron micrographs were taken at random from the body of the corpus callosum immediately above the horizontal longitudinal fibers of the body of the fornix, and from the rostral part of the dorsal hippocampal commissure immediately caudo-ventral to these fibers. Negatives were digitized at 600 dpi using a UMAX scanner, and visualized with MCID 4.0 image analysis software. For each myelinated axon, automatic edge detection software was used to determine the axonal area in transverse section, from which the diameter of a circle of equivalent area was calculated (axon diameter). Myelin sheath thickness was measured directly in 5 places around the sheath at locations where it was sectioned transversely rather than obliquely, and a mean value calculated. Total fiber diameter was calculated by adding double the mean sheath thickness to the axon diameter. Mean values for these parameters were calculated for each animal. In addition a G ratio was calculated for each myelinated axon by dividing axon diameter by total fiber diameter, and then a mean value for all axons was calculated for each brain region in each animal. These means were used to calculate a group mean for G ratio in each region at each time point (19). In addition, for each photomicrograph from which measurements were made, the total numbers of myelinated and non-myelinated fibers were counted, and total proportions determined for each animal and as a mean proportion from each group of animals. Between groups G ratio data were analysed by one-way ANOVA followed by Dunnett's test using the normal mice as the controls. Separate within groups comparisons of G ratio were by ANOVA followed by Bonferroni's multiple comparison test of selected pairs. In addition, following best-fit analysis that suggested that the data were most appropriately described by a first order equation, a linear regression analysis of myelin sheath thickness on axon diameter was performed for each mouse.

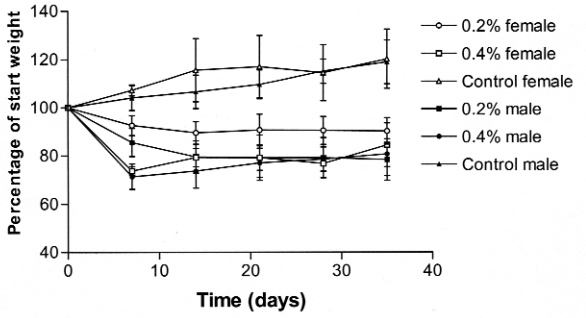

Figure 2. Weight changes during intoxication with 0.2% or 0.4% cuprizone in normal 10-week-old age-matched male and female C57Bl/6 mice. 0.4% groups reverted to 0.2% cuprizone after 3 weeks.

Results

0.2% cuprizone is a more suitable dosage in terms of mouse morbidity and weight loss than 0.4% cuprizone. Weight curves for the cuprizone-treated mice are shown in Figure 2. Whilst the control animals continued to gain weight throughout the course of the experiment, the weights of animals in the 0.4% groups dropped precipitously, by up to 40% of starting weights. In addition, these animals exhibited marked clinical signs including listlessness, anorexia, ataxia, and tremors, and several died within the first 3 weeks. Consequently, from the third week, all animals were returned to a 0.2% dose for the remainder of the experiment, and weights stabilized or recovered, with a parallel improvement in clinical

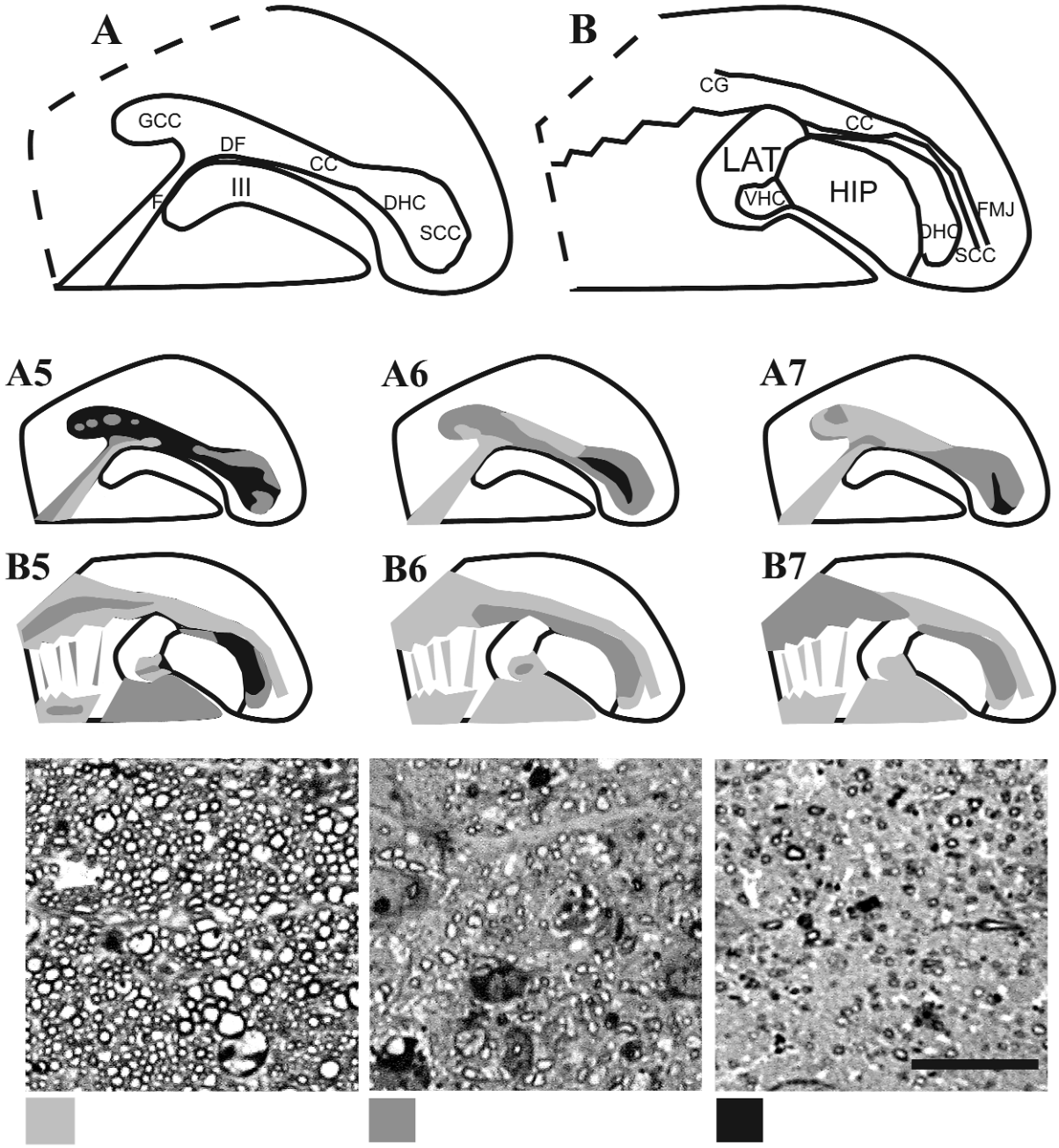

Figure 3. Changes in myelination in forebrain white matter tracts after cuprizone administration. Anatomical features of sagittal (**A**) and para-sagittal (**B**) sections, with the distribution of myelin changes indicated schematically for each group of mice after 5 weeks of cuprizone administration (A5, B5) and one (A6, B6) and two (A7, B7) weeks after cuprizone withdrawal. Micrographs below show representative areas corresponding to the shading indicated above. CC corpus callosum, CG cingulum, DF dorsal fornix, DHC dorsal hippocampal commissure, F fornix, FMJ forceps major corpus callosum, GCC genu corpus callosum, HIP hippocampus, LAT lateral ventricle, SCC splenium corpus callosum, VHC ventral hippocampal commissure, III third ventricle. (Bar = 10 μm)

signs. As a result, all further experiments used a dose rate of 0.2% cuprizone.

Distribution of cuprizone-induced demyelination is anatomically variable. Considerable variation in the myelination of different anatomical regions of the corpus callosum was apparent at all three time points examined. Because of the small diameter of many of the fibers, myelinated and remyelinated axons could not be readily distinguished with the light microscope (in contrast to the situation in the cerebellar peduncles, where the predominant large fiber size makes comparisons of sheath thickness much easier). From the lesion maps constructed for each mouse, an "aggregate map" was constructed which represented the global distribution of myelin across all of the mice (Figure 3). Extensive areas of homogeneous demyelination were rare at this dose, and even in areas where demyelination predominated, it was not uncommon to see patches of myelinated axons, or more widely dispersed single myelinated axons. In general, the splenium and dorsal hippocampal commissure regions were most severely affected, with fewest myelinated axons, and the greatest degree of cellular infiltration. Changes extended patchily forwards along the body of the corpus callosum into the genu. However, large areas of the central, rostral and ventral genu, together with the radiating portion of the corpus callosum in the para-sagittal plane, were largely spared. When the sagittal and para-sagittal sections from each time point were given a myelination rank by a single observer, there was no significant difference in ranking between the 2 sections. This implies that in addition to the differences in susceptibility of different areas of white matter tracts within a single animal, there was significant and consistent variation between animals in the overall susceptibility of areas of the corpus callosum and adjacent tracts to cuprizone-induced demyelination. In addition, we observed that severe hydrocephalus and myelin oedema occurred in one animal and persisted after cuprizone withdrawal, even at the 0.2% dose, and made assessment of myelination status impossible.

In order to confirm that the variability we had observed was typical, we repeated the experiment using age-matched male mice of the same genotype, and a protocol in which mice received twice daily tamoxifen for 5 days only, starting at the time of cuprizone withdrawal. We observed similar variability amongst the 4 mice in each group at both 6 and 7 weeks (data not shown).

The rostral cerebellar peduncle is not susceptible to demyelination with low dose cuprizone. Previous studies have clearly established that the larger diameter myelinated axons of the rostral cerebellar peduncle are a good substrate for the analysis of remyelination (5, 6, 17). Despite these documented advantages, and reports alluding to the demyelination of the rostral cerebellar peduncle with a 0.2% dose of cuprizone in C57Bl/6 mice (15, 24), recent studies have used the corpus callosum as the substrate for analysis. Consequently, we examined the rostral cerebellar peduncle in our mice in order to establish whether it would be useful for evaluation. We found that the rostral cerebellar peduncle did not show evidence of either significant demyelination or an associated infiltration of macrophages into myelinated tracts in this region (not shown).

Variability in the response and small axon diameter makes assessment of the progress of early remyelination difficult. The heterogeneity of severity and distribution of myelin alterations across the corpus callosum, and the predominant small fiber diameter in this region, limited the discrimination of primary and secondary myelination with the resolution afforded by light microscopy. Consequently, we used electron microscopy to enable a more detailed ultrastructural examination of selected areas. We examined all 4 normal animals as a baseline for comparison in 2 anatomical areas. One, in the body of the corpus callosum, corresponded to the area used in previous reports (22). The second, the dorsal hippocampal commissure, was chosen on the basis that the light microscopic survey suggested that axons in this area showed the most consistent demyelination and vigorous cellular reaction to it in cuprizone-treated animals. Since we suspected that the variability in response to cuprizone may reflect a qualitative as well as a quantitative difference in myelination, we selected the top, middle and bottom ranking animals from the 6- and 7-week groups for analysis, as representatives of the spectrum of changes observed (Figure 4).

A survey of the selected areas by electron microscopy confirmed earlier impressions of myelination status obtained by examination of resin sections by light microscopy. In particular it was apparent on visual inspection that the thickness of the myelin surrounding myelinated axons during these early periods in some mice was similar to that in normal mice (Figure 4). In addition, most of these axons were of small diameter, and there was overlap between the diameters of myelinated and unmyelinated axons. This meant that it was not

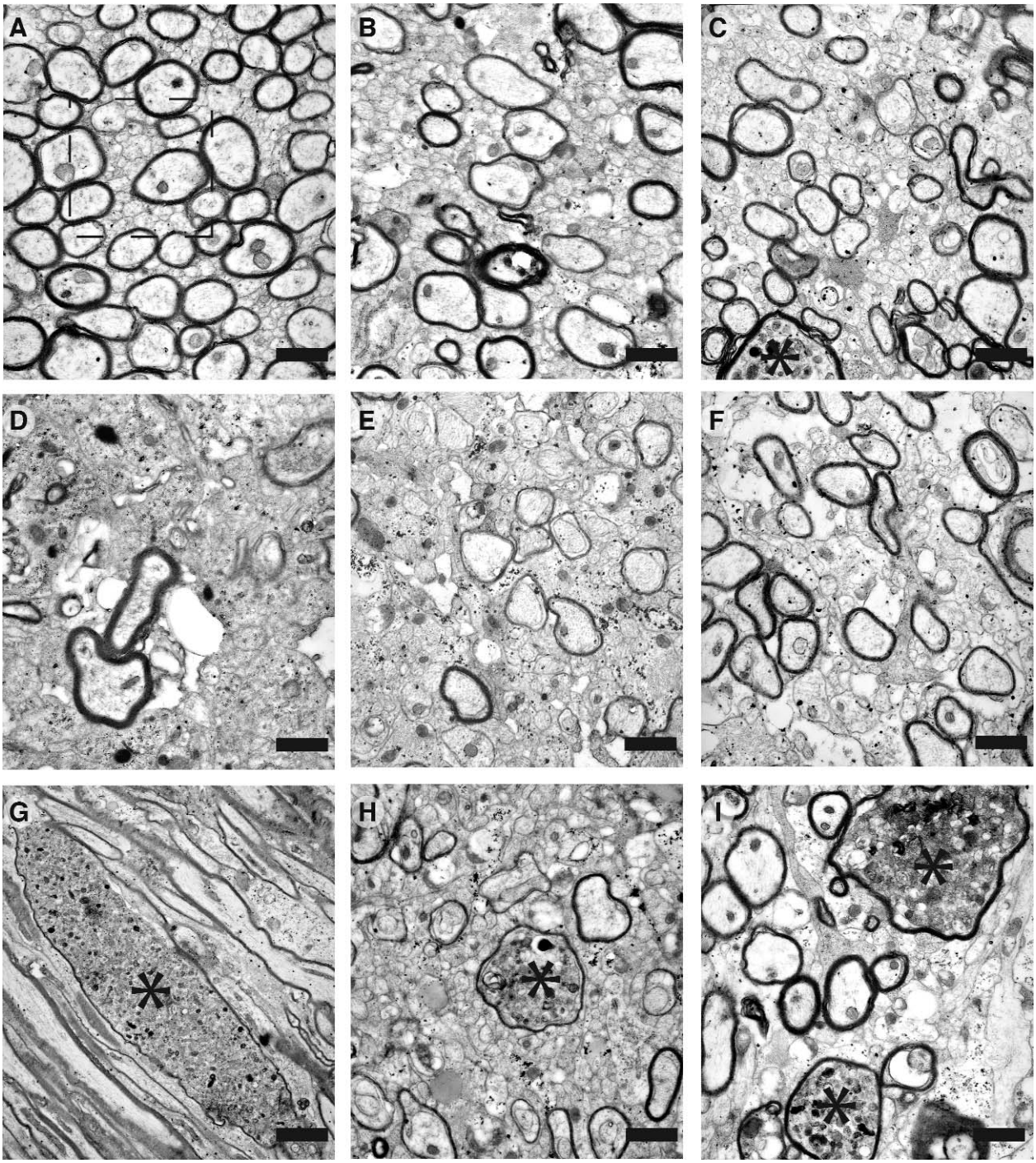

Figure 4. Electron micrographs of corpus callosum of normal (**A**), and cuprizone-treated (**B-I**) mice, allowed to recover for one (**B, E, H**) and two (**C, F, I**) weeks. **B** (G ratio = 0.77) and **E** (G ratio = 0.88), and **C** (G ratio = 0.8) and **F** (G ratio = 0.83) demonstrate representative areas of the body of the corpus callosum. Myelin sheaths of variable thickness are present even after 5 weeks of cuprizone (**D**). Axonal pathology (asterisks) was observed after 5 weeks of cuprizone (**G**) and after one or 2 weeks' recovery (**H, I**). Note the small unmyelinated axons in normal corpus callosum (dashed box in **A**). (Bar = 1 μm)

clear whether these axons were in fact residual primary myelinated axons, or newly remyelinated axons, particularly in the light of the variability in distribution of the cuprizone response we had noted. In order to address this more objectively, further axonal and myelin parameters were quantified by morphometry in the 2 anatomical areas.

Changes in the proportions of myelinated and unmyelinated axons follow expected trends, but show pronounced variation between animals. The results for the proportions of myelinated and unmyelinated axons are presented in Figure 5. These were derived by counting the total numbers of axons with and without myelin sheaths contained within all of the randomly selected electron micrographs from each animal in which axons were measured. There are significant proportions of small non-myelinated fibers in both selected areas in the normal animals. Although there is a trend towards a gradual increase in the proportion of myelinated axons over the course of 2 weeks, there is also marked variability in the proportions between different animals in the same experimental groups, and overlap between the proportions which are found at consecutive time points.

Group mean G ratios do not change significantly during the early stages of remyelination. The main purpose of morphometry was to clarify whether ultrastructural examination was an unequivocal method of distinguishing populations of axons with primary myelin or remyelination, when light microscopy was unable to do so. Data derived from the morphometric analysis of 2 distinct corpus callosum regions are presented in Figure 6, which also includes data derived from the untreated age-matched C57Bl/6 mice. No significant changes in mean G ratios were observed between groups during the first 2 weeks of remyelination after cuprizone withdrawal in the body of the corpus callosum, or in the dorsal hippocampal commissure, when compared to normal mice. In addition, there were no significant differences between groups in axon diameter, myelin thickness, or fiber diameter. In contrast, within groups, there were significant differences in the mean G ratios between different animals, even within the control group (data not shown), suggesting that inter-animal variability was masking any trend towards an increase in G ratio that might occur as remyelinated axons were invested with thinner myelin sheaths than their control counterparts. Whilst in the control group the variability appeared to be attributable predominantly to differences in myelin thickness on similarly sized axons, in the

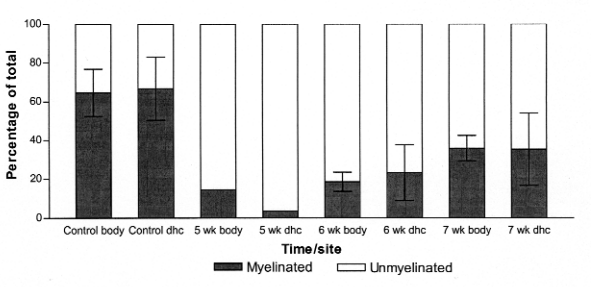

Figure 5. Proportions of myelinated and unmyelinated axons measured in normal and cuprizone-treated mice at the end of five weeks of cuprizone, and after one or 2 week's recovery. Body = body of corpus callosum, dhc = dorsal hippocampal commissure.

6- and 7-week groups the variability was in some cases attributable to differences in myelin thickness alone and in others to differences in both axon diameter and myelin thickness together. These results suggested that inherent variability in both the anatomy of the system and the response of both axons and myelin to cuprizone could be obscuring changes attributable to early processes of remyelination.

Regression analysis reveals a complex relationship between axon diameter and myelin sheath thickness during the early stages of remyelination. In order to investigate in more detail the relationship between axon diameter and myelin thickness in these samples, we performed a linear regression of myelin thickness on axon diameter for each animal, treating each anatomical area separately. Results are presented in Figure 7. They suggest that the relationship between axon diameter and myelin sheath thickness was not straightforward. For a number of animals, the slope of the regression line did not differ significantly from zero, indicating that axon diameter did not predict myelin thickness. In other animals, particularly in the 6- and 7-week groups, the slope did differ significantly from zero, but the value of R^2 (correlation coefficient) was small (range 0.15 to 0.17 for 6-week groups, 0.072 to 0.5 for 7-week groups), indicating that the majority of the variability in myelin sheath thickness was not explained by variation in axon diameter in most cases. Even amongst the normal animals, there was one animal in which there was no apparent relationship between axon diameter and myelin thickness. These data suggest that at these anatomical locations and with the morphometric criteria laid out above, myelin thickness did not vary with axon diameter in a predictable manner in the early regenerative response to 0.2% cuprizone intoxication.

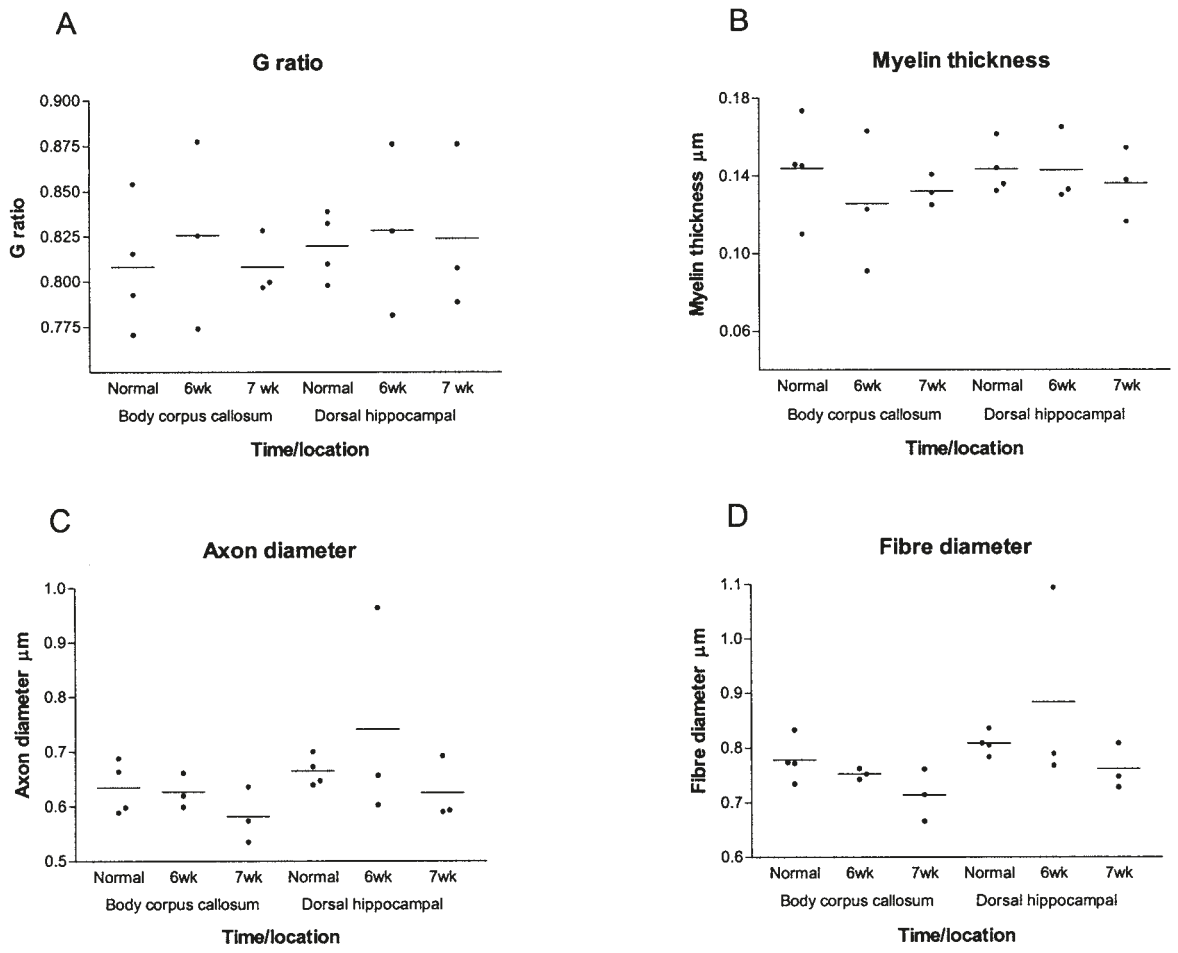

Figure 6. Morphometric data derived from ultrastructural measurements in normal and cuprizone-treated mice, as described in methods. **A**) G ratio, **B**) Myelin thickness, **C**) Axon diameter, **D**) Total myelinated fiber diameter. There are no significant differences between the group mean values for any parameter in either location or at either time. Each point represents the mean value from at least 50 individual axonal measurements.

Axonal pathology is a significant subcomponent of the response to cuprizone. An additional feature was the presence of swollen dystrophic axons in sections from all time points in cuprizone-treated animals (Figure 4). Such axons were frequently larger than those surrounding them, and usually comprised a wrinkled but intact myelin sheath surrounding axons distended by a mixture of materials of variable electron density and distended vacuolar structures. Occasionally axons were shrunken with denser grey granular contents. Dystrophic axons were never seen in normal mice, and were scarce in the two 5-week animals, although the amount of oedema resulted in markedly reduced axon densities. In order to gain some indication of the number of dystrophic axons, a single photomicrograph (5000×) from each area (body of corpus callosum or dorsal hippocampal commissure) was randomly selected from each animal. The number of dystrophic axons was expressed as a percentage of the total number of myelinated axons in the areas examined. No dystrophic axons were observed in the selected micrographs from normal or 5-week cuprizone-treated animals. For the 6-week animals, the percentages of dystrophic axons were 6.1 ± 2.4% (body) and 0 ± 0% (commissure). In the 7-week animals, the figures were 4.4 ± 0.7% (body) and 1.1 ± 1.0% (commissure).

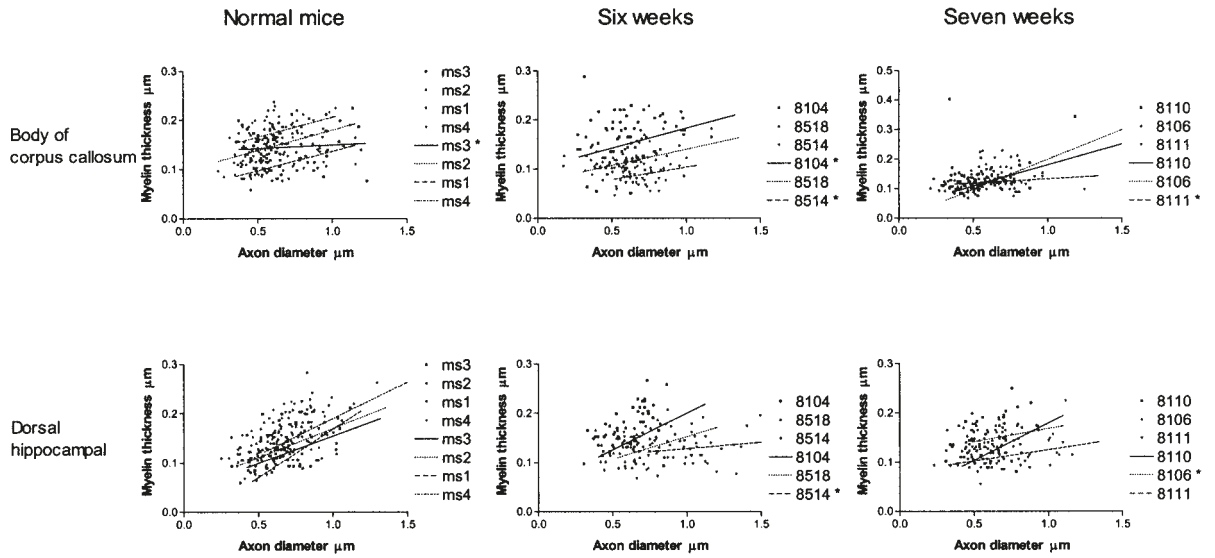

Figure 7. Regression data of myelin thickness on axon diameter following cuprizone intoxication. Individual data points for each axon are plotted together with the line of best fit obtained by linear regression. Data are plotted separately for each region. Asterisks denote that the slope of the regression line is not significantly different to zero, implying that there is no relationship between axonal diameter and myelin thickness.

Discussion

In this study we have attempted to validate protocols and baseline information for the accurate recognition and quantification of the early stages of remyelination in the central nervous system. We evaluated the earliest stages of the remyelination response following cuprizone demyelination of the corpus callosum of adult mice as a potential model in which to investigate factors influencing the differentiation and maturation of oligodendrocyte progenitors recruited to areas of demyelination. Our choice of mouse strain and cuprizone dose was by necessity limited by both the genetic phenotype of the available animals, and by local ethical constraints relating to animal use. The approach seemed promising however, since a number of recent papers have used the cuprizone model under similar circumstances to compare the effects of a range of growth factors and inflammatory mediators on remyelination in transgenic mice (1-3, 11, 20, 21, 23). As a result of our experiences we suggest that such constraints may have a significant bearing on the use of variants of this model in remyelination studies.

Parameters that we chose to investigate were the extent of myelination, the proportion of myelinated axons regaining a myelin sheath, and most importantly, the rate at which new myelin sheaths were laid down on demyelinated axons. In order to achieve this we undertook a survey of the distribution of myelin changes in mice following a 5-week period of 0.2% cuprizone intoxication and during 2 further weeks of remyelination after cuprizone was withdrawn. We analyzed changes in terms of distribution, axon proportion and G ratio (the ratio of fiber diameter to the diameter of fiber plus myelin sheath). G ratio cannot be measured for completely denuded axons, but as the myelin sheath is laid down in a sequential fashion wrap by wrap, it would be expected that a newly remyelinated fiber would have an increased G ratio when compared with a normally myelinated fiber of equivalent diameter. The measurement of G ratio by electron microscopy is a well-established technique in remyelination biology.

Our observations suggest that the demyelination and subsequent remyelination response to 0.2% cuprizone in this group of mice was not as uniform, as complete or as easy to interpret as expected. Individual animals showed differences in overall susceptibility, but in addition there was anatomical variation within white matter tracts in individual mice. The caudal regions of the corpus callosum were more susceptible than the rostral parts to demyelination at this dose, although even within affected areas patches of myelinated axons remained. When we attempted to distinguish between primary myelin and remyelination using ultrastructural examination of defined regions we found that we were unable to make such a distinction on the basis of a set of morphometric parameters. Furthermore, the data also suggested that it was often difficult to demonstrate a clear

relationship between axonal diameter and myelin thickness in the population of myelinated axons examined in these locations.

One explanation for these observations is an inherent variability in the cuprizone response at this low dose. In addition there are the possibilities of bias introduced by the size distributions of myelinated axons remaining after cuprizone treatment (fibers are characteristically small, and the range of diameters is narrow), by inconsistency in the distribution of axons of different sizes across the corpus callosum and by the limitations of our sampling method. It is possible that the fiber sizes and distributions in the corpus callosum vary between mice, since there are differences in axon diameters between our study and those of others (19, 25). Others have reported a bimodal distribution of myelinated and unmyelinated fiber diameters, with significant overlap between the 2 populations (25). Furthermore, there are strain differences in the composition of the corpus callosum itself (13), and changes in myelin to axon ratios with aging (12), all of which can further complicate interpretation of studies. One factor which might impinge on changes in the average G ratio early in remyelination is the downward shift in the distribution of axonal diameters under the influence of cuprizone which has been previously reported (19). Although not directly comparable with our data, these authors found that G ratios measured either following 6 weeks of cuprizone (no recovery) or after 6 weeks of cuprizone and 4 weeks recovery were not significantly different from controls, suggesting that they may have been observing a phenomenon similar to that which we recorded. The earliest studies on cuprizone-induced demyelination (5) also found that the relationship between axon diameter and myelin sheath thickness was lost during the earliest part of the recovery phase.

The generation of conditional transgenic mice may require the combination of a number of independently segregating alleles within the same animal. This makes backcrossing to genetic uniformity difficult and time-consuming. Part of the variability which we observed in our experiment could therefore be explained by differences in backcrossing between animals, either through a differential response to cuprizone (10, 15, 17, 22), or through differences in the development and anatomy of the corpus callosum (13) .

Possible solutions to these problems might include a significant increase in the numbers of animals required for such studies. Sampling of additional axons may help to increase the accuracy of individual means and reduce bias. Although increasing the dose of cuprizone may help to increase the reproducibility of the response, this may not be feasible as a result of the unacceptable clinical problems and weight loss which we and others have described (15). Even if an increased dose of cuprizone (eg, 0.3%) proves acceptable in a particular mouse population, the within-group variabilities observed may still be sufficient to prevent potential differences between groups reaching significance (1).

Cuprizone intoxication has generally been considered to be largely oligodendrocyte specific. However, dystrophic axons were observed in early ultrastructural studies using 0.5% cuprizone fed for 8 weeks to weanling mice (14). Others have found axons to be largely normal in similar circumstances (4, 17). Axonal pathology following 0.2% cuprizone intoxication receives little attention in recent reviews (22). Necrotic axons were observed in a study of axonal caliber in which a significant shift in axonal size distributions was noted (19), but they were not thought to be significant. In the absence of comparative data on the prevalence of such axons in previous studies, we are unable to compare our results directly. Nevertheless, we have shown that a small but significant population of the myelinated axons are dystrophic in this location with a 0.2% dose of cuprizone. Whether such changes are transient or result in axonal death is unclear, as is the overall effect of such axonal pathology in the absence of a detailed (and laborious) analysis of total axon number. Such an effect would be in addition to the hydrocephalus and myelin oedema observed in a significant proportion of animals by others (7, 16, 17), and as seen here and in subsequent experiments in our laboratory. It seems unlikely that tamoxifen administration accounts for the axonal pathology since it has been reported in the absence of tamoxifen and no such effects have been reported for the drug itself previously.

In conclusion, our observations suggest that during early remyelination following cuprizone, the G ratio measurements in defined areas of central nervous system white matter follow unexpected patterns. Furthermore, the variability in the demyelination response within acceptable dose limits and the predominance of small fiber diameters in the corpus callosum hamper the discrimination of remyelination by both light and electron microscopy. Despite this, some areas of the corpus callosum do appear to demyelinate more reliably than others, and it is possible that by restricting analyses to these regions and by performing dose titrations in different strains of mice the difficulties could be overcome. Nevertheless, our experiences would suggest that the model is not ideal for studying the earliest differentiation phases of remyelination, and that even in long-term

studies of remyelination outcome the ultrastructural confirmation of the presence of definitive remyelination (as opposed to residual myelin) ought to be undertaken on a case-by-case basis.

Acknowledgments

The technical expertise of Anil Kalupahana and Mike Peacock in the preparation and photography of sections for light and electron microscopy, and of Dr Rachel Woodruff in generating the dose-weight measurements, is gratefully acknowledged. MFS holds a Wellcome Trust Research Training Fellowship. US is supported by the Swiss National Science Foundation and the National Center of Competence in Research "Neural Plasticity and Repair."

References

1. Armstrong RC, Le TQ, Frost EE, Borke RC, Vana AC (2002) Absence of fibroblast growth factor 2 promotes oligodendroglial repopulation of demyelinated white matter. *J Neurosci* 22:8574-8585.
2. Arnett HA, Hellendall RP, Matsushima GK, Suzuki K, Laubach VE, Sherman P, Ting JP (2002) The protective role of nitric oxide in a neurotoxicant-induced demyelinating model. *J Immunol* 168:427-433.
3. Arnett HA, Mason J, Marino M, Suzuki K, Matsushima GK, Ting JP (2001) TNFalpha promotes proliferation of oligodendrocyte progenitors and remyelination. *Nat Neurosci* 4:1116-1122.
4. Blakemore WF (1973) Demyelination of the superior cerebellar peduncle in the mouse induced by cuprizone. *J Neurol Sci* 20:63-72.
5. Blakemore WF (1973) Remyelination of the superior cerebellar peduncle in the mouse following demyelination induced by feeding cuprizone. *J Neurol Sci* 20:73-83.
6. Blakemore WF (1974) Remyelination of the superior cerebellar peduncle in old mice following demyelination induced by cuprizone. *J Neurol Sci* 22:121-126.
7. Carlton WW (1967) Studies on the induction of hydrocephalus and spongy degeneration by cuprizone feeding and attempts to antidote the toxicity. *Life Sci* 6:11-19.
8. Chang A, Nishiyama A, Peterson J, Prineas J, Trapp BD (2000) NG2-positive oligodendrocyte progenitor cells in adult human brain and multiple sclerosis lesions. *J Neurosci* 20:6404-6412.
9. Chang A, Tourtellotte WW, Rudick R, Trapp BD (2002) Premyelinating oligodendrocytes in chronic lesions of multiple sclerosis. *N Engl J Med* 346:165-173.
10. Elsworth S, Howell JM (1973) Variation in the response of mice to cuprizone. *Res Vet Sci* 14:385-387.
11. Gao X, Gillig TA, Ye P, D'Ercole AJ, Matsushima GK, Popko B (2000) Interferon-gamma protects against cuprizone-induced demyelination. *Mol Cell Neurosci* 16:338-349.
12. Godlewski A (1991) Morphometry of myelin fibers in corpus callosum and optic nerve of aging rats. *J Hirnforsch* 32:39-46.
13. Gozzo S, Renzi P, D'Udine B (1979) Morphological differences in cerebral cortex and corpus callosum are genetically determined in two different strains of mice. *Int J Neurosci* 9:91-96.
14. Hemm RD, Carlton WW, Welser JR (1971) Ultrastructural changes of cuprizone encephalopathy in mice. *Toxicol Appl Pharmacol* 18:869-882.
15. Hiremath MM, Saito Y, Knapp GW, Ting JP, Suzuki K, Matsushima GK (1998) Microglial/macrophage accumulation during cuprizone-induced demyelination in C57BL/6 mice. *J Neuroimmunol* 92:38-49.
16. Kesterson JW, Carlton WW (1970) Aqueductal stenosis as the cause of hydrocephalus in mice fed the substituted hydrazine, cuprizone. *Exp Mol Pathol* 13:281-294.
17. Ludwin SK (1978) Central nervous system demyelination and remyelination in the mouse: an ultrastructural study of cuprizone toxicity. *Lab Invest* 39:597-612.
18. Ludwin SK (1980) Chronic demyelination inhibits remyelination in the central nervous system. An analysis of contributing factors. *Lab Invest* 43:382-387.
19. Mason JL, Langaman C, Morell P, Suzuki K, Matsushima GK (2001) Episodic demyelination and subsequent remyelination within the murine central nervous system: changes in axonal caliber. *Neuropathol Appl Neurobiol* 27:50-58.
20. Mason JL, Suzuki K, Chaplin DD, Matsushima GK (2001) Interleukin-1beta promotes repair of the CNS. *J Neurosci* 21:7046-7052.
21. Mason JL, Ye P, Suzuki K, D'Ercole AJ, Matsushima GK (2000) Insulin-like growth factor-1 inhibits mature oligodendrocyte apoptosis during primary demyelination. *J Neurosci* 20:5703-5708.
22. Matsushima GK, Morell P (2001) The neurotoxicant, cuprizone, as a model to study demyelination and remyelination in the central nervous system. *Brain Pathol* 11:107-116.
23. McMahon EJ, Cook DN, Suzuki K, Matsushima GK(2001) Absence of macrophage-inflammatory protein-1alpha delays central nervous system demyelination in the presence of an intact blood-brain barrier. *J Immunol* 167:2964-2971.
24. Morell P, Barrett CV, Mason JL, Toews AD, Hostettler JD, Knapp GW, Matsushima GK et al (1998) Gene expression in brain during cuprizone-induced demyelination and remyelination. *Mol Cell Neurosci* 12:220-227.
25. Sturrock RR (1980) Myelination of the mouse corpus callosum. *Neuropathol Appl Neurobiol* 6:415-420.
26. Wolswijk G (1998) Chronic stage multiple sclerosis lesions contain a relatively quiescent population of oligodendrocyte precursor cells. J Neurosci 18:601-609.
27. Wolswijk G (2002) Oligodendrocyte precursor cells in the demyelinated multiple sclerosis spinal cord. Brain 125:338-349.
28. Woodruff RH, Franklin RJM (1999) Demyelination and remyelination of the caudal cerebellar peduncle of adult rats following stereotaxic injections of lysolecithin, ethidium bromide, and complement/anti-galactocerebroside: a comparative study. Glia 25:216-228.

.